

Absolute Cross Section Versus Energy of the $\text{Cu}^{63}(\gamma, n)$ and $\text{Cu}^{63}(\gamma, 2n)$ Reactions*

ARTHUR I. BERMAN AND KARL L. BROWN

Department of Physics and High Energy Physics Laboratory, Stanford University, Stanford, California

(Received June 29, 1954)

Experimental values were found for the absolute cross section of both $\text{Cu}^{63}(\gamma, n)$ and $(\gamma, 2n)$ reactions versus quantum energy from threshold to 36 Mev. Statistical and systematic errors were limited by the use of (a) the direct electron beam of the Stanford 36-Mev linear accelerator, which produced bremsstrahlung immediately before and within the copper foils under bombardment, (b) an electron-beam collector which recorded the total accumulated charge in the incident flux, (c) a 4π scintillation counter which measured the activity of the resultant Cu^{62} and Cu^{61} , and (d) electroplated foils of separated Cu^{63} isotope.

The cross-section curves of the two reactions are similar—both rise rapidly to a maximum value about 6 Mev above threshold and then fall to zero almost as rapidly. The integrated cross sections were found to be 0.55 ± 0.03 and 0.081 Mev-barn for the (γ, n) and $(\gamma, 2n)$ reactions, respectively. The $(\gamma, 2n)$ threshold is 20.0 ± 0.5 Mev. A precision of 0.5 percent was attained in the relative (γ, n) activation points and 5 percent in the absolute cross section integrated over energy. The corresponding errors in the $(\gamma, 2n)$ data were 5 and 20 percent; the latter value includes the effect of a 10 percent uncertainty in the currently published data on the electron-capture to positron-emission ratio of Cu^{61} .

I. INTRODUCTION

THE number of publications relating to photoneuclear reactions has become so extensive in the past few years that no attempt is made here to provide a complete reference to this voluminous material, as an introduction to this research. There are, however, several articles of a review nature which should lead the reader to most of the published work in this field.¹⁻³

The $\text{Cu}^{63}(\gamma, n)\text{Cu}^{62}$ cross section has been studied in detail by several investigators,⁴⁻¹¹ and the $\text{Cu}^{63}(\gamma, 2n)$ cross section has been studied by Montalbetti *et al.*² The present experiment differs from the others principally in the energy range covered by the experiment and in the method of determining the photon flux initiating the reactions. With one exception,⁹ the results of all the previous measurements of the $\text{Cu}^{63}(\gamma, n)$ and $(\gamma, 2n)$ absolute cross sections were dependent upon the calculated response of an r meter or ionization chamber, whereas Krohn and Shrader used a pair spectrometer calibrated against the theoretical and experimental cross section for the photodisintegration of the deuteron.

In this experiment, the external electron beam of the Stanford 36-Mev linear accelerator¹² was used directly to activate a stack of Cu foils. The beam passed successively through a thin Cu correcting foil (explained in detail later), a relatively thick radiator, and a second identical thin foil, and then directly into a "Faraday

cup" electron collector which permitted a precise measurement of the accumulated charge in the incident electron flux. From knowledge of the integrated charge and the Bethe-Heitler theory,¹³ the effective photon spectrum passing through the second thin foil can be determined to good precision.

The number of photoneutrons ejected from the copper foil was determined in this experiment by counting the residual radioactivity of the Cu^{62} and Cu^{61} isotopes (resulting from the $\text{Cu}^{63}(\gamma, n)\text{Cu}^{62}$ and the $\text{Cu}^{63}(\gamma, 2n)\text{Cu}^{61}$ reactions) with a 4π scintillation counter. To avoid interference from extraneous activities, the $(\gamma, 2n)$ cross section was evaluated by using electroplated foils of Cu^{63} separated isotope.

II. EXPERIMENTAL TECHNIQUE

The Stacked-Foil Method

When photoneuclear reactions are produced by quanta which are created within and immediately preceding the material under study, one is able to establish almost precisely the photon flux initiating the reactions. This flux is determined from knowledge of the incident electron-beam intensity and of Bethe-Heitler bremsstrahlung theory¹³ (modified slightly to account for the finite radiator thickness).¹⁴

Unfortunately, the accuracy of this technique is modified somewhat by the existence of a background effect, namely, the similar reactions induced by the virtual quanta identified with the electromagnetic field of the moving electrons. These are in contradistinction to the bremsstrahlung quanta which are created by electrons as they decelerate in matter. Although the cross section for the electronuclear effect is only about one percent of the photoneuclear process¹⁵ for thin targets, there may be several hundred electrons striking

* The research reported in this document was supported jointly by the U. S. Navy (Office of Naval Research) and the U. S. Atomic Energy Commission.

¹ K. Strauch, *Ann. Rev. Nuclear Sci.* **2**, 110 (1953).

² Montalbetti, Katz, and Goldemberg, *Phys. Rev.* **91**, 659 (1953).

³ A. I. Berman, *Am. J. Phys.* **22**, 277 (1954).

⁴ G. C. Baldwin and G. S. Klaiber, *Phys. Rev.* **73**, 1156 (1948).

⁵ B. C. Diven and G. M. Almy, *Phys. Rev.* **80**, 407 (1950).

⁶ L. Katz and A. G. W. Cameron, *Can. J. Phys.* **29**, 518 (1951).

⁷ P. R. Byerly and W. E. Stephens, *Phys. Rev.* **83**, 54 (1951).

⁸ L. I. Newkirk, *Phys. Rev.* **86**, 249 (1952).

⁹ V. E. Krohn and E. F. Shrader, *Phys. Rev.* **87**, 685 (1952).

¹⁰ K. Strauch, *Phys. Rev.* **81**, 973 (1951).

¹¹ Marshall, Rosenfeld, and Wright, *Phys. Rev.* **83**, 305 (1951).

¹² R. Post and N. Shiren, *Rev. Sci. Instr.* (to be published).

¹³ H. Bethe and W. Heitler, *Proc. Roy. Soc. (London)* **A146**, 93 (1934).

¹⁴ R. Wilson, *Proc. Phys. Soc. (London)* **A66**, 638 (1953).

¹⁵ K. L. Brown and R. Wilson, *Phys. Rev.* **93**, 443 (1954).

the sample for every effective bremsstrahlung photon produced, and so the two effects may be quite comparable in magnitude. To some extent, the difficulty can be lessened by extending the thickness of the radiator; however, a point is soon reached where the degeneration of both electron and photon energies in the mass of the radiator introduces a sizable uncertainty in the calculated photon flux.

The number of unwanted reactions—be they induced by the electrons, neutrons, or stray gamma radiation entering with the electrons—can be measured conveniently by placing a foil, equivalent to the sample, in front of the radiator and observing the reaction yield. Thus, the electron beam passes successively through a thin correcting foil, a relatively thick radiator, and a (second identical) thin rear sample foil. Of course, the front foil, being of finite thickness, acts as its own radiator, producing a small amount of “self-induced” photonuclear reactions, which are equivalent (except for a degeneration factor) to those induced similarly in the rear foil. The net difference in reaction yield (corrected for photon and electron degeneration) between the rear and front foils is then due only to bremsstrahlung quanta produced in the radiator and front foil, the sum being the “effective radiator.”

In this experiment, the reaction yield is measured by determining the radioactivity of the ten-minute copper-62 and three-hour copper-61 nuclei which results from the (γ, n) and $(\gamma, 2n)$ processes, respectively, in copper-63. Both radioisotopes emit positrons, whose end-point energies are 2.9 and 1.3 Mev, respectively.

Naturally occurring copper is composed of isotopes 63 and 65 in the proportion 69:31. Of all competing photon-induced activities which can occur in these isotopes, only the $\text{Cu}^{65}(\gamma, n)$ reaction appears to be of any consequence. This twelve-hour copper-64 activity conflicts so strongly with the weak three-hour $(\gamma, 2n)$ activity to be measured, that it was necessary to perform the $\text{Cu}^{63}(\gamma, 2n)$ experiment with highly-enriched copper-63 foils. Oxide containing 99.4 percent copper-63 was borrowed from Oak Ridge. Smooth foils were then electroplated from a weak (about 0.1 normal) nitric-acid solution on a polished, stainless-steel anode (rotated at one rps to stir the solution and insure uniformity); the foils were then easily stripped. Foils ranging in thickness from 3 to 16 mg/cm^2 and totaling 130 mg/cm^2 were made. They were reduced in a hydrogen atmosphere and weighed immediately. A beta-ray gauge was constructed to determine their uniformity, which in nearly all cases varied not more than 2 percent in standard deviation.

Incident Electron-Flux Measurement

The electrons from the Stanford 36-Mev linear accelerator were magnetically analyzed and collimated in high vacuum so that a fairly uniform beam of $\frac{1}{8}$ -inch by $\frac{5}{8}$ -inch cross section entered the foils. The foil holder was mounted in air at the entrance to a Faraday-cup

electron collector.¹⁶ This consisted of a graphite cylinder bored with a deep hole and backed by lead as illustrated in Fig. 1. The electrons are attenuated primarily by ionization in the graphite, and any photons produced are effectively absorbed by the lead. The lip at the front of the graphite serves two purposes. First, it narrows the aperture to a size more nearly consistent with the beam dimensions and hence helps to prevent loss of secondary particles. Second, those few electrons which would strike the inner surface of the graphite near the aperture at grazing angles and eject secondaries are forced to enter the carbon block at a more nearly normal angle of incidence, and thus eject fewer secondaries. The purpose of the ring magnet is to deflect the low-energy secondary particles generated at the base of the cup back into the collector. Thus, the emergent beam, with all its secondary products, is contained within the integrator; the net accumulated charge is therefore a direct measure of the number of electrons collected.

To test the efficiency of the collector, the beam was monitored with a hydrogen ion chamber preceding the foils, and the cup was biased through a range of +900 to -900 volts. Upon extrapolating the resultant collection yield (normalized to constant beam intensity) to saturation voltages, it was observed that the influence of low-energy secondary particles resulted in a change in total charge accumulation of less than ± 2 percent. To verify that charged particles resulting from the electron shower were effectively trapped by the cup, a further test was made. The ionizing radiation leaving the end and sides of the cup was measured by calibrated x-ray film and also by a Victoreen ionization thimble. From this, it was possible to calculate the maximum loss of charged particles. This predicted that the total number of particles lost was less than one-half of one percent of the incident flux. Inasmuch as both electrons and positrons are generated in the cup, and the film and Victoreen thimble are insensitive to charge polarity, the actual loss is expected to be even less. This result is further verified by the work of Kantz on the penetration depth of electron-induced showers.¹⁷

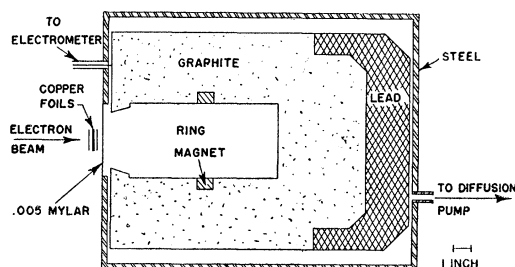


FIG. 1. Experimental arrangement showing the Faraday cup electron collector and bombardment position of the foils.

¹⁶ A more complete description of this collector and its associated circuitry is discussed in a paper to be submitted to the *Review of Scientific Instruments* by K. L. Brown and G. W. Tauffest.

¹⁷ A. D. Kantz, Stanford High Energy Physics Laboratory Technical Report HEPL-17, May 1954 (unpublished).

TABLE I. $\phi(\epsilon, \epsilon_M)/\phi_0$ in Mev⁻¹ for 0.025-radiation-length copper.

$\epsilon \setminus \epsilon_M$	10	12	14	16	18	20	22	24	26	28	30	32	34	36	38	40
9	399	725	905	1037	1138	1220	1289	1348	1399	1442	1479	1512	1542	1570	1596	1621
11		346	590	730	824	897	957.5	1009	1054.5	1092.5	1126	1156	1183.5	1208.5	1232	1254
13			297	488	611	690	749	797	838.5	873.5	904.5	932	957	980	1001	1020.5
15				255	425	529	597	646.5	686.5	720	749	774	797	817.5	836.5	853.5
17					220	370	456.5	512.5	554.5	588	616	640	661	679.5	696.5	711.5
19						193	321	393	442	478	506	529	549	566.5	582	595.5
21							172	297	360.5	404	434.5	458	477	493	507	518.5
23								158	264	325.5	365	392.5	413	429.5	443	454
25									145	249	306.5	343	367	385.5	400	410.5
27										135	230	283	316	338	353.5	364.5
29											126	211	260	290.5	310	323
31												118	198	245	273	290.5
33													110	187	229	254
35														102.5	175.5	215.5
37															95	164
39																88

These facts demonstrate the reliability of the cup as an absolute beam-monitor in the energy range of the accelerator. The ion-chamber monitor was used also to correlate the beam emerging from the foils with the incident beam at the various primary-electron energies. An observed difference was caused by the primary-electron beam scattering foil electrons into the collector. This necessitated a correction of from 2.5 percent at 36 Mev to essentially zero at 12 Mev. Similar scattering in the 0.005-inch Mylar foil window of the collector required a correction of 2.3 percent (calculated from the Møller scattering formula).

The charge from the collector was accumulated on a condenser in an electrometer unit. A slide-back voltage was continuously applied through an electronic feedback circuit which maintained a zero net voltage across the Faraday-cup collector. Fluctuations in beam intensity during the run would introduce serious errors unless corrected for; for example, an increase in intensity is more serious near the end of a run than near the beginning, as activity induced near the beginning will be more likely to have decayed before the counting period starts. To offset this, a technique used by Snowdon was used.¹⁸ A high resistance was placed across the condenser so that the accumulated charge leaked off at the rate of decay of the reaction being studied.

Photon-Flux Calculation

The Bethe-Heitler formula, including screening, as integrated over all angles of photon emission was employed to calculate the number of photons in each quantum-energy interval for an infinitesimal thickness of radiator.¹³ This formula suffers from the fact that the Born approximation was used in its derivation. Thus, at the high-energy end of the spectral distribution, where the recoil electron has practically zero kinetic energy, the formula is invalid. Further, the over-all cross section is subject to a possible error which increases with Z .

¹⁸ S. C. Snowdon, Phys. Rev. 78, 299 (1950).

In an attempt to relieve the first difficulty, the bremsstrahlung cross section was adjusted by a multiplying factor calculated by Sommerfeld for the nonrelativistic formula,¹⁹ which causes the cross section to be finite rather than zero at the cut-off energy.

The second difficulty is alleviated by noting the recent work of Bethe *et al.*²⁰ which substantiates the validity of the Bethe-Heitler formula for large momentum transfers. This is not true of the pair production cross section, as has been shown by experiment.²¹ Nevertheless, with a copper radiator as was used in this experiment, even if the error in the Bethe-Heitler bremsstrahlung formula were as large as the pair-production error, the net error to this experiment would not exceed one percent.

In order to adjust the Bethe-Heitler formula for the finite thickness of the radiator, it was necessary to account for the degeneration of the electrons and photons. Wilson's formula¹⁴ was used for this purpose. At the high-energy end, errors resulting from the application of this formula become more serious than the uncertainty in the use of the Sommerfeld factor. These calculated values are tabulated in Table I. The bremsstrahlung cross section is given as $\phi(\epsilon, \epsilon_M)/\phi_0$ in Mev⁻¹ for 0.025-radiation-length copper (0.3325 g/cm²). $\phi_0 = r_0^2/137$, where $r_0 = 2.818 \times 10^{-13}$ cm (classical electron radius); $\phi(\epsilon, \epsilon_M)$ = bremsstrahlung cross section per copper nucleus, integrated over all angles of emission, in an energy range ϵ and $\epsilon + d\epsilon$, per incident electron of kinetic energy ϵ_M . These values should be multiplied by $(Z + \delta)/Z$ to include the contribution to bremsstrahlung production by interactions with the field of atomic electrons. An approximate value of $\delta = 1$ is used in this work.

It was necessary to know with some degree of accuracy the electron kinetic energy and therefore the maximum photon energy incident on the foils. At the

¹⁹ W. Heitler, *The Quantum Theory of Radiation* (Clarendon Press, Oxford, 1936), p. 171.

²⁰ H. A. Bethe and L. C. Maximon, Phys. Rev. 93, 768 (1954); Davies, Bethe, and Maximon, Phys. Rev. 93, 788 (1954).

²¹ A. I. Berman, Phys. Rev. 90, 210 (1953).

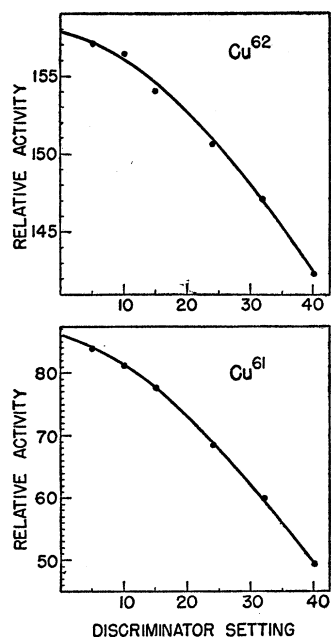


FIG. 2. Relative activity *vs* discriminator setting for a foil 6.9 mg/cm² thick.

exit point of the accelerator the electron beam was deflected by the field of an electromagnet, and a fraction, depending on the geometry, was transmitted through collimators to the foils. The energy calibration was obtained as follows. The relation between the field and magnet current was found to 0.1 percent accuracy by inserting a rotating coil into the magnetic field and comparing the induced voltage obtained with that from a permanent magnetic field. This function was then normalized to an absolute value by observing the magnet current at the threshold of the (γ, n) reaction in Cu^{63} and C^{12} . The former value, 10.61 Mev, is a result of a precise measurement of Birnbaum,²² while the latter, 18.71 Mev, is found from nuclear mass spectrometer values.²³ Throughout the experiment, the magnet current, measured with a potentiometer, was reversed, raised, and lowered in a fixed manner to provide assurance that all settings followed a fixed hysteresis loop. Furthermore, the magnet was operated well below the saturation level resulting in an almost linear function of energy *versus* magnet current, which again assured reproducibility of the energy settings. The energy resolution of the electrons incident on the foils was found to be 1.5 percent by deflecting the beam with a second magnet through fine slits.

Measuring the Radioactivity

The activity induced in the front and rear foils was measured with a 4π scintillation counter. The foil was

sandwiched between two flat anthracene crystals, 1-inch square and $\frac{1}{8}$ -inch thick, backed by two DuMont 6292 photomultipliers. The natural-copper foils used in the (γ, n) runs were $1\frac{1}{4}$ -inch diameter disks 40 mg/cm² thick, while the enriched foils were $\frac{1}{2}$ -inch \times $\frac{3}{4}$ -inch strips totaling 65 mg/cm². The cross section of the beam was shown by film exposure to be completely contained in the foils. Hence, any positrons of the induced activity which escaped the foils with finite energy would most certainly be absorbed in the anthracene and cause a light pulse to be produced. So long as the foil was reasonably centered between the crystals, it was impossible to detect changes in the counting rate as a function of the foil's position. However, every effort was made to duplicate the runs precisely by giving close attention to constants of the experiment, such as foil position, both in the beam and in the counter. The photomultiplier outputs were equalized and then connected in parallel. The pulses were fed successively into a Los Alamos-type 501 amplifier and Berkeley decimal scaler. Very small pulses, commensurate with the noise level, were eliminated by a discriminator. To account for the proportion of pulses lost, an extrapolation of a plot of activity *versus* discriminator setting was made for a thin foil (6.9 mg/cm²). In Fig. 2 this plot is shown for both Cu^{61} and Cu^{62} . The result was not at variance with the expected Fermi distribution, if one allows a 50 percent tolerance in the calibration of the discriminator. This calibration was made by using the 167-keV end-point energy of S^{35} . During the experimental runs, a discriminator setting of 32 volts was chosen to reject unwanted low-energy activity and to decrease the background counting rate. The counter background was 0.6 count per second.

It was found that for thin foils the fraction lost by discrimination barely varies with foil thickness so that the result of the extrapolation can be assumed to be that for a foil of zero thickness. The 2–3 mil thickness of the foils used in the regular runs permitted some self-absorption to occur. Fortunately, in 4π geometry, a plot of specific activity *versus* thickness is semi-logarithmic, and the extrapolation to zero thickness can be made without difficulty. This is shown in Fig. 3. The self-absorption factors found were essentially equal to those calculated from the self-absorption coefficients of Baker and Katz.²⁴

Measurements of the half-lives of the two isotopes were made with the 4π counter. The results are 9.73 ± 0.02 minutes for Cu^{62} , and 3.32 ± 0.03 hours for Cu^{61} . The latter result is in agreement with other workers, while the former is up to 7 percent lower than some of the previously published values. The shorter half-life was measured after bombarding the enriched foils below the $(\gamma, 2n)$ threshold. Actually, ordinary copper could have been used in this determination provided the discriminator had been set high enough to eliminate

²² M. Birnbaum, Phys. Rev. **93**, 146 (1954).

²³ See, for example, E. Segrè, editor, *Experimental Nuclear Physics* (John Wiley and Sons, Inc., New York, 1953), p. 745.

²⁴ R. G. Baker and L. Katz, *Nucleonics* **11**, 14 (1953).

the competing Cu⁶⁴ activity. At any rate, the discriminator was set at a sufficiently high value to lower the background count. Paired runs of 45 minutes each were compared and the initial counting rate was chosen low enough to prevent uncertainties in the dead-time from seriously affecting the result. Other paired runs of 20-minutes and 2-minute duration were taken at different intervals with respect to the initial bombardment time and all results fall within the statistical error stated. This value of half-life was used to recompute the dead-time of the scalars (6.0 ± 0.5 microseconds at the 32 discriminator setting) at fast counting rates, which in turn allowed a more sensitive computation of the half-life to be made at moderate counting rates.

III. EXPERIMENTAL RESULTS

Activation Curves

Activation points were taken at 2-Mev intervals. Smaller intervals, which would permit fine rather than coarse structure determinations of the cross section, would require a higher-energy resolution of the incident electron beam, and further knowledge about the bremsstrahlung energy distribution near cutoff. For the (γ, n) measurements, five sets of front and rear foils of the ordinary copper were used. Five runs of 200 seconds each were made at a given energy and then repeated at a later date with the foil positions interchanged. Each foil was counted for 100 seconds and counting rates were of the order of 1000 counts per second. An additional run was made with the enriched foils to check on possible interference from activities induced in the copper-65 isotope in ordinary copper; in particular, the Cu⁶⁵($\gamma, 3n$) reaction, which would produce an excess of 10-minute Cu⁶². Since no excess was observed in the natural copper relative to the enriched foils, it was concluded that up to 36 Mev, activity from this reaction must be less than one percent of the Cu⁶³(γ, n) activity. The Cu⁶⁵($\gamma, 2n$) leads to the stable isotope Cu⁶³ and

therefore is not detectable by this experimental technique.

Experimental Corrections

The ($\gamma, 2n$) runs, two at each energy, were made exclusively with the enriched foils. The subtraction of counts due to competing reactions and to residual activity from previous runs was usually made without difficulty. Normally (for counting rates in excess of 20 counts per second) the competing Cu⁶⁴ activity was evaluated by counting it after the decay of the three-hour Cu⁶¹ activity and then correcting by extrapolating back to the original Cu⁶⁴ activity. However, at lower counting rates, although the Cu⁶⁴ activity still represented a significant correction to the observed Cu⁶¹ activity, the usual procedure could not be followed as the amount of the Cu⁶⁴ activity remaining after decay of the Cu⁶¹ was so small as to be completely obscured by the natural counter background. In this event, a 2½-hour run of constant beam intensity was made and high counting rates were assured by using a ¼-inch lead converter. By following the decay of the sample over an extensive period, the resultant activities could be separated and the initial counting-rate ratio of Cu⁶²:Cu⁶⁴ determined. Since the Cu⁶³(γ, n)Cu⁶² and Cu⁶⁵(γ, n)Cu⁶⁴ cross sections occur at essentially the same effective quantum energy—well below the region of the Cu⁶³($\gamma, 2n$)Cu⁶¹ cross section—it seemed reasonable to assume the above ratio to be essentially independent of energy above the ($\gamma, 2n$) threshold. This was indeed found to be the case. Thus, in the regular low-counting rate ($\gamma, 2n$) runs, the expected Cu⁶² activity was deduced from a knowledge of the average beam intensity and from the already determined Cu⁶³(γ, n)Cu⁶² activation curve. This, combined with the above ratio, then determined the expected Cu⁶⁴ background activity.

Multiple scattering of the primary electrons in the foils increases the effective path lengths of the bremsstrahlung quanta and electrons in the rear foil relative to the first. A correction for this was applied which varied from 4 to 0.4 percent from 12 to 36 Mev.²⁵ A further correction resulted from the fact that the electrons, which contribute nearly 80 percent of the background activity in the rear foil, are degenerated in energy while traversing the radiator. The remaining background consists of approximately 20 percent stray gamma-ray induced activity (as determined by magnetically removing the electrons before they strike the foils, and observing the resultant activity), and about 1 percent neutron-induced activity (about equal in each foil). Both the gamma and neutron backgrounds were precisely accounted for in each bombardment by the foil-subtraction process. Except for a slight degeneration correction, which can be made with only an order-of-magnitude knowledge of the background, it should be recalled that subtracting the front-foil activity from

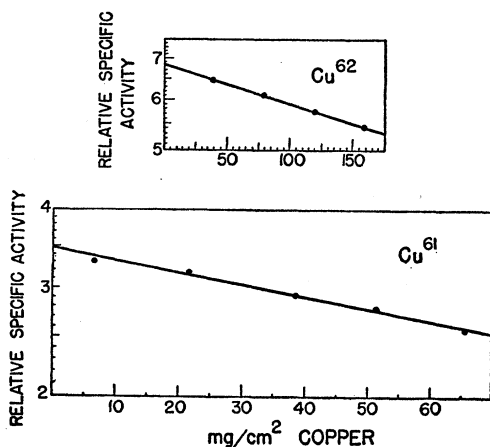


FIG. 3. Self-absorption curves in 4π geometry of Cu⁶² and Cu⁶¹ activities.

²⁵ K. L. Brown, Ph.D. dissertation, Department of Physics, Stanford University, June, 1953 (unpublished).

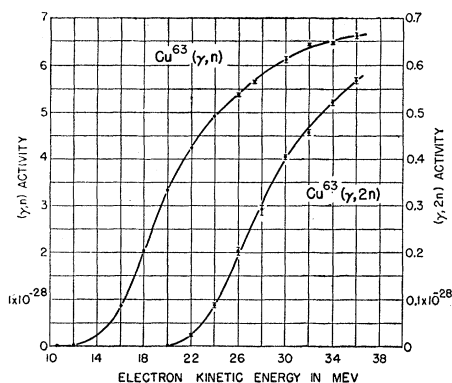


FIG. 4. Activations per Cu^{63} nucleus per electron per cm^2 incident on a 0.025-radiation-length (0.3325 g/cm^2) copper radiator for the $\text{Cu}^{63}(\gamma, n)$ and $(\gamma, 2n)$ reactions.

the rear-foil activity eliminates the effect of any induced background which is the same in both foils. The validity of this method is borne out by the results of runs on the same set of foils at the same energy but on different occasions. The activity in the front and rear foils normalized to the integrated beam was not consistent from run to run (indicating different gamma backgrounds), whereas the difference in activity reproduced to better than 0.5 percent. Activity induced by foil electrons scattered from rest into an energy region above threshold was calculated to be negligible. The electron-degeneration correction was obtained through the use of the activation curve of the electron-induced reaction derived from the photonuclear activation curve and the photonuclear-electronuclear activation ratio of Brown and Wilson.¹⁵ From this, and the theoretical value of the average electron-energy degeneration expected, the corrected rear-foil electron activation was computed.

The corrected activation curves for the two reactions are plotted in Fig. 4. The average standard deviation of the individual points is about 0.5 percent.

Cross-Section Curves

The cross sections at odd-Mev points were computed by applying the photon-difference method⁶ to the activation curves using bremsstrahlung distributions calculated at even-Mev intervals for a 0.025-radiation-length copper radiator. The yield formula is

$$Y(\epsilon_M) = n_e N_r N \int_{\epsilon_T}^{\epsilon_M} \phi(\epsilon, \epsilon_M, t) \sigma_\epsilon d\epsilon, \quad (1)$$

where ϵ = quantum energy in Mev, ϵ_M = maximum quantum energy equal to electron kinetic energy, $Y(\epsilon_M)$ = total activated nuclei in the foil corresponding to a maximum quantum energy ϵ_M , n_e = number of incident electrons, N_r = effective number of radiator nuclei per cm^2 , N = number of nuclei per cm^2 in the sample, $\phi(\epsilon, \epsilon_M, t)$ = cross section in cm^2 per Mev interval for radiator of thickness t , and σ_ϵ = reaction cross section in cm^2 at energy ϵ .

In the determination of the absolute cross section for the $(\gamma, 2n)$ process, the activation was adjusted for the number of Cu^{61} disintegrations which proceed through electron-capture, by the electron-capture to positron-emission ratio of Cook²⁶ of 0.47. This value is subject to an error of about 10 percent. The result is in excellent agreement with that obtained for the electron-capture to positron-emission ratio calculated theoretically from the decay scheme.²⁷ A 655-keV gamma ray is present in 20 percent of the Cu^{62} disintegrations, and a 284-keV gamma ray in 3 percent. For the anthracene crystals in the counter of 0.5-cm effective thickness, Compton interactions require a correction to the measured activity amounting to 1.0 ± 0.3 percent.

The copper-62 nucleus decays also partially by electron capture. A theoretical lower limit to the electron-capture to positron-emission ratio is 2.1 percent assuming that all disintegrations proceed directly to the ground state. On the other hand, the small amount of branching which may occur would increase the ratio by two or three times. However, as the precise decay scheme is not yet known, the lower limit was used in stating the final activation and cross-section values.

The cross sections are shown in Figs. 5 and 6. The conclusion may be drawn that in these reactions at the measured energies, the process is more reasonably described by a compound-nucleus model in which the neutrons are evaporated as a statistical fluctuation, than by a model in which the neutrons are ejected by a direct interaction with the incident photon. In the latter case, one would expect the cross section to decrease more slowly past the maximum.²⁸ The expected ratio of the $(\gamma, 2n)$ cross section to the cross section of all reactions in which at least one neutron is emitted may be calculated from the statistical model

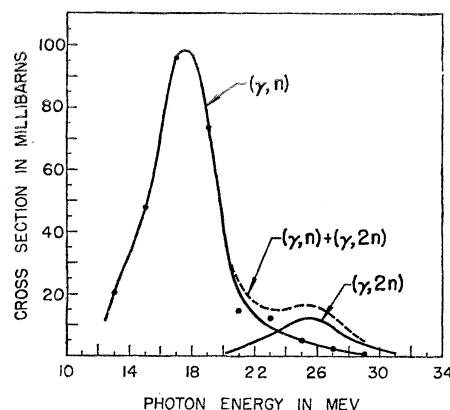


FIG. 5. $\text{Cu}^{63}(\gamma, n)$ and $(\gamma, 2n)$ cross sections.

²⁶ C. S. Cook, Phys. Rev. **83**, 462 (1951).

²⁷ Owen, Cook, and Owen, Phys. Rev. **78**, 686 (1950); R. Bouchez, Physica **18**, 1171 (1952). The authors are indebted to Professor W. Meyerhof for his information on the latest available data on the electron-capture ratios.

²⁸ E. D. Courant, Phys. Rev. **82**, 703 (1951); C. Levinthal and A. Silverman, Phys. Rev. **82**, 822 (1951).

of Weisskopf and Ewing²⁹ as

$$\begin{aligned} \sigma(\gamma, 2n) / [\sigma(\gamma, n) + \sigma(\gamma, 2n) + \sigma(\gamma, pn) + \sigma(\gamma, 3n) + \dots] \\ = 1 - [1 + (a/E)^{1/2}(E - E_b)] \\ \times \exp[-(a/E)^{1/2}(E - E_b)], \quad (2) \end{aligned}$$

where $a = 2.2 \text{ Mev}^{-1}$ for copper, $E = \epsilon - \epsilon_T(\gamma, n) = \epsilon - 10.6 \text{ Mev}$, and $E_b = \epsilon_T(\gamma, 2n) - \epsilon_T(\gamma, n) = 20 - 10.6 = 9.4 \text{ Mev}$.

Table II compares the calculated values with the results of this experiment at several quantum energies. The (γ, pn) cross section could readily account for the observed discrepancy.

The observed ($\gamma, 2n$) threshold is $20.0 \pm 0.5 \text{ Mev}$. This is not quite at the maximum energy for the (γ, n) reaction, as might be expected on an evaporation model, probably because of competition from the (γ, pn) reaction. Judging from the small amount of information available on other isotopes,² this latter cross section is expected to be of the same order of magnitude as the ($\gamma, 2n$) cross section.

The cross sections integrated over all energies up to 35 Mev for the (γ, n) and ($\gamma, 2n$) reactions are 0.55 and 0.081 Mev-barn, respectively. The same values were found either from the area of the curves or from the values of the yield at 36 Mev and the bremsstrahlung cross section at the mean cross-section energy. The theoretical integrated cross sections for all reactions in copper were found by Levinger and Bethe³⁰ to be 0.95 (1+0.8x) Mev-barns for Cu⁶³. The value of x, the fraction of neutron-proton exchange force quoted in the paper, is 0.55, so that the integrated cross section

TABLE II. $\sigma(\gamma, 2n) / [\sigma(\gamma, n) + \sigma(\gamma, 2n) + \dots]$ calculated from the statistical model and compared with the experimental result of $\sigma(\gamma, 2n) / [\sigma(\gamma, n) + \sigma(\gamma, 2n)]$.

Energy (Mev)	Theory	Experiment
21	0.08	0.13
23	0.36	0.43
25	0.58	0.71
27	0.73	0.79

TABLE III. Integrated cross section for the reaction Cu⁶³(γ, n).

$\sigma(\gamma, n)$ (Mev-barns)	Reference
0.60	5
0.63	6
0.76	10
0.77 ± 0.15	11
0.55 ± 0.03	this paper

²⁹ V. F. Weisskopf and D. H. Ewing, Phys. Rev. **57**, 472 (1940).

³⁰ J. S. Levinger and H. A. Bethe, Phys. Rev. **78**, 115 (1950).

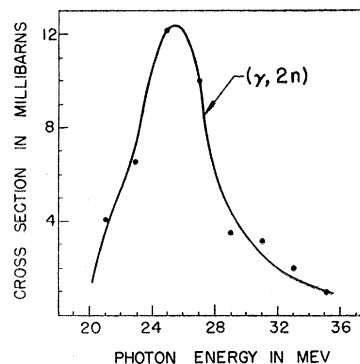


FIG. 6. Cu⁶³($\gamma, 2n$) cross section.

would then be 1.35 Mev-barns. This is considerably higher than the 0.63 Mev-barn found experimentally for the (γ, n) and ($\gamma, 2n$) integrated sum. The inequality may be due to (a) the presence of competing cross sections, notably the (γ, pn) and (γ, p), or (b) the probable increase of the cross sections at several hundred Mev.

In Table III, the (γ, n) cross section is compared with those of other workers.

The error in the values of the integrated cross section may be estimated as 5 percent for the (γ, n) reaction and 20 percent for the ($\gamma, 2n$) reaction. In the first reaction, an error of 1 to 2 percent arises from the calculation of the thick-target bremsstrahlung distribution. The precision of the integrated value would be sensitive only to the part of the bremsstrahlung distribution between 12 and 24 Mev, which is known to good accuracy for primary-electron energies in the neighborhood 30–36 Mev. The limit of accuracy of the electron collector is 2 percent, and fluctuations in foil mass per unit area constitute the remainder of the major errors. In the ($\gamma, 2n$) absolute determination, aside from the slightly poorer counting statistics, an additional error occurs due to the significant self-absorption of the lower-energy beta particles in the thicker foils. Furthermore, the published uncertainty in the ratio of electron-capture to positron-emission is about 10 percent.²⁶

ACKNOWLEDGMENT

The authors wish to thank Professor W. K. H. Panofsky, under whose direction this research was carried out. Acknowledgment is made of the assistance on several phases of this work given by Dr. W. C. Barber and Wayland George. We also wish to thank many other members of the Hansen Laboratories staff who have contributed to the completion of this research; in particular, C. Newton, D. D. Reagan, C. Hsieh, and J. Helmer, who have helped in the development of the Faraday-cup integrator.